

Dual-wavelength mode-locked laser based on evanescent field interaction with MAX phase saturable absorber

A.A.A. Jafry^{1,2,*}, N. Kasim², and S.W. Harun³

¹ Foundation/Diploma, School of Pre-University Studies, Taylor's College Lakeside Campus, No. 1, Jalan Taylor's, 47500 Subang Jaya, Selangor Darul Ehsan

² Department of Physics, Faculty of Science, Universiti Teknologi Malaysia, 81310 Skudai, Johor, Malaysia

³ Department of Electrical Engineering, University of Malaya, 50603 Kuala Lumpur, Malaysia

E-mail: afiqarifst@gmail.com

Received: 04 April 2021. Accepted: 31 May 2021. Published: 15 July 2021

To cite this article: A.A.A. Jafry et al (2021) Journal Fotonik 2 2 8

Abstract

For the first time, we proposed a dual-wavelength laser generation with a titanium aluminum carbide (Ti_3AlC_2) as a saturable absorber in an erbium-doped fiber laser cavity. The saturable absorber device based on the MAX phase Ti_3AlC_2 deposited onto D-shaped fiber has successfully triggered a dual-wavelength laser centered at 1533 nm and 1557 nm. The elemental composition and vibrational modes of the saturable absorber were analyzed by using energy-dispersive x-ray spectroscopy and Raman spectroscopy for chemical analysis. We also captured a strong saturable absorption of 2% and a non-saturable absorption of 49.2% at the 1.55- μm , confirmed its ability to generate pulses in the near-infrared wavelength spectrum. The dual-wavelength laser owns a pulse width of 280 ns, a repetition rate of 1.887 MHz, and a signal-to-noise ratio of ~63 dB. By varying the laser diode pump from 62-90 mW, a stable dual-wavelength laser was generated with the highest single pulse energy of 2.33 nJ, which corresponded to the output power of 4.4 mW. This demonstration shows the potential of MAX phase Ti_3AlC_2 as a saturable absorber in an all fiber-based laser cavity.

Keywords

evanescent field, MAX phase, dual-wavelength laser, mode-locked, D-shaped fiber

1. Introduction

In the past two decades, avalanche research has confirmed the nonlinear optical properties of many materials and its application as a short-pulsed laser (SPL) generator [1]. Since Graphene was discovered in 2004 by Novoselov et al. [2], a few of the carbon analogues were utilized as a material to initiate pulsed laser in a fiber laser cavity [3, 4]. The generation of laser in the form of optical pulses was realized based on the saturable absorption mechanism. As light enters a fiber laser cavity and hits the material known as saturable absorber (SA), the electron inside the SA absorbed the photons and it causes the electron to jump towards the excited state. Finally, all the quantum states were filled, and no more electron could make an inter-band transition, this obeys the Pauli blocking principle where two or more electrons cannot occupy the same quantum state simultaneously. As a result, the electrons returned to the lower energy state, which causes them to release the photons in the form of optical pulses; thus, the SPL generated. Such-laser was essential for a variety of industrial and scientific applications including, corrective eye surgery, soft/hard tissue ablation, steel cutting technology, and several others. Hence, a great deal of interest was conducted, all-aimed to improve the lasers' performance, for instance, by selecting a material with excellent saturable absorption properties, the pulse duration of the laser can be shortened [5]. As of now, a multitude of materials was used to generate the SPL. Most materials can be categorized into a few categories such as, carbon-based materials, transition metal dichalcogenides, topological insulators, metal oxide, metal nanoparticles, organic materials, ternary metal carbides/nitrides (MXene), etc [6, 7].

For a material to qualify as SA, it needs to satisfy the following criteria. First, a material with a small electronic bandgap that allowed the emission of light in the near-infrared region. It needs to own the linear absorption that contributes to the substantial modulation depth at the working wavelength. Also, a high optical damage threshold is desirable to ensure the material

did not damage at a high pumping power of the laser. Until now, the two-dimensional (2D) materials mentioned above had fulfilled the first two specifications; however, the last criteria still needed attention. Among the 2D allotropes, MXene attracts immense attention among scientists and engineers, and this is due to its astounding saturable absorption properties. Begin with the works on the ultrafast laser generation using MXene $Ti_3C_2T_x$ by Jiang et al. [8], as of today, more than 20 publications related to MXene as a broadband pulse generator was published [9, 10]. MXene is a 2D ternary metal carbide or/and nitride that originates from the MAX phase material. It mimics the electronic properties of metal and the physical characteristics of ceramic, making it useful for a variety of applications. Therefore, without any doubt, it was useful for the photonics application as well, and its potential for ultrafast laser applications has already been exploited. On the contrary, the works regarding its bulk counterparts, MAX phase is still limited.

Ti_2AlC is the first material from the MAX phase family, which proved to be an efficient SA in the 1.55- μm region. Lee et al. generate a Q-switched laser with the shortest pulse width of 4.88 μs [11]. In this regard, authors investigate the optical properties of Ti_3AlC_2 by confirming the adequate saturable absorption of the thin film Ti_3AlC_2 with a 2% modulation depth obtained from the linear absorption of 3 dB. However, the laser's stability at a high pump power cannot be maintained with this thin-film structure. As established, the thin-film with different polymer as a host suffers from a photo-darkening effect, which causes the mechanical and physical breakdown to the SA device, and it makes the tip of fiber-ferrule burned. In this regard, this problem was solved with a different SA implementation method in a fiber laser cavity. Here, the development of the SA device with Ti_3AlC_2 MAX phase deposited onto the D-shaped fiber (MAX-DSF) was demonstrated. The obtained MAX-DSF SA owns a saturable absorption of 2%, the non-saturable absorption of 49.2%, and it was able to generate a dual-wavelength (DWL) mode-locked laser with a pulse width of 280 ns. The laser operates stably within the pump power of 62 to 90 mW at the operating wavelengths of 1533 nm and 1557 nm. To the best of authors' knowledge, this is the first demonstration of dual-wavelength laser generation with a MAX phase deposited onto the D-shaped fiber in an all fiber-based laser cavity.

2. Preparation, characterization, and nonlinear absorption spectrum of Ti_3AlC_2

The SA device was synthesized based on the liquid casting method, which offers a straightforward preparation procedure than most of the other techniques [12, 13]. The essential ingredients were polyvinyl alcohol (PVA), deionized (DI) water, and the Ti_3AlC_2 powder. They were stirred and ultrasonicated to obtain a mixture of liquid SA. First, the PVA solution was synthesized by stirring 1 g of its powder with 120 mL of DI water. The temperature was set at 200 °C with a stirring speed of 300 rpm. Later, the as-prepared solution was mixed with the Ti_3AlC_2 powder by using stirring and ultrasonication. The amount of the powder used was 10 mg, while the PVA solution used was 40 mL. They were stirred for 24 hrs, followed by the ultrasonication for 2 hrs. A dusty-like particle presence at the bottom of the beaker proved the success of the process. Only the supernatant was used as a SA, and it was deposited onto the D-shaped fiber. A 3 μL solution was used as a SA, dropped on the D-shaped fiber with the EDFL cavity operates in the CW regime. Finally, the MAX-DSF SA was left to dry for 3 hrs at room temperature.

The SA's characteristics were confirmed with the energy-dispersive x-ray spectroscopy (EDS), Raman spectroscopy, and variable-pressure scanning electron microscopy (VP-SEM). As shown in Figure 1 (a), the EDS spectrum revealed four main elements that exist in the composition of Ti_3AlC_2 . Titanium, as the main element, owns a 73.2% weight, while only 10.5% weight of aluminum captured from the measurement. The carbon and oxygen represent 9.3% and 7% of the total elemental compositions. Further validation of the vibrational modes

was determined by using UniDRON, Confocal microscope Raman spectroscopy. It unveils the spectrum in Figure 1 (b) with six Raman peaks, equivalent to the theoretical prediction by Presser et al [14]. The first four peaks belong to the active phonon vibration modes of Ti_3AlC_2 , and the peaks located at the end of the spectrum represent the disordered carbon in the composition. The peak at the wavenumber of 171 cm^{-1} , 407 cm^{-1} , 517 cm^{-1} , and 638 cm^{-1} was assigned to the Raman modes of E_g , E_{2g} , E_{1g} , and A_{1g} . The last two peaks located at the 1318 cm^{-1} and 1281 cm^{-1} represents the D and G bands of disordered carbon. Those two measurements verify the presence of Ti_3AlC_2 in the developed SA. As depicted in Figure 1 (c), the surface morphology captured with VP-SEM indicates the consistent particle size of Ti_3AlC_2 powder. Finally, the balanced-twin detector technique unveils the nonlinear absorption spectrum of the MAX-DSF. As illustrated in Figure 1 (d), the SA owns a saturable absorption of 2%, a non-saturable absorption of 49.2%, and a saturable intensity (I_{sat}) of 2.68 MW/cm^2 . A stable 3.6 ps mode-locked at the 1558 nm was used as the laser source for the measurement. Thus, the developed SA device can generate a pulsed laser in the 1.55- μm region.

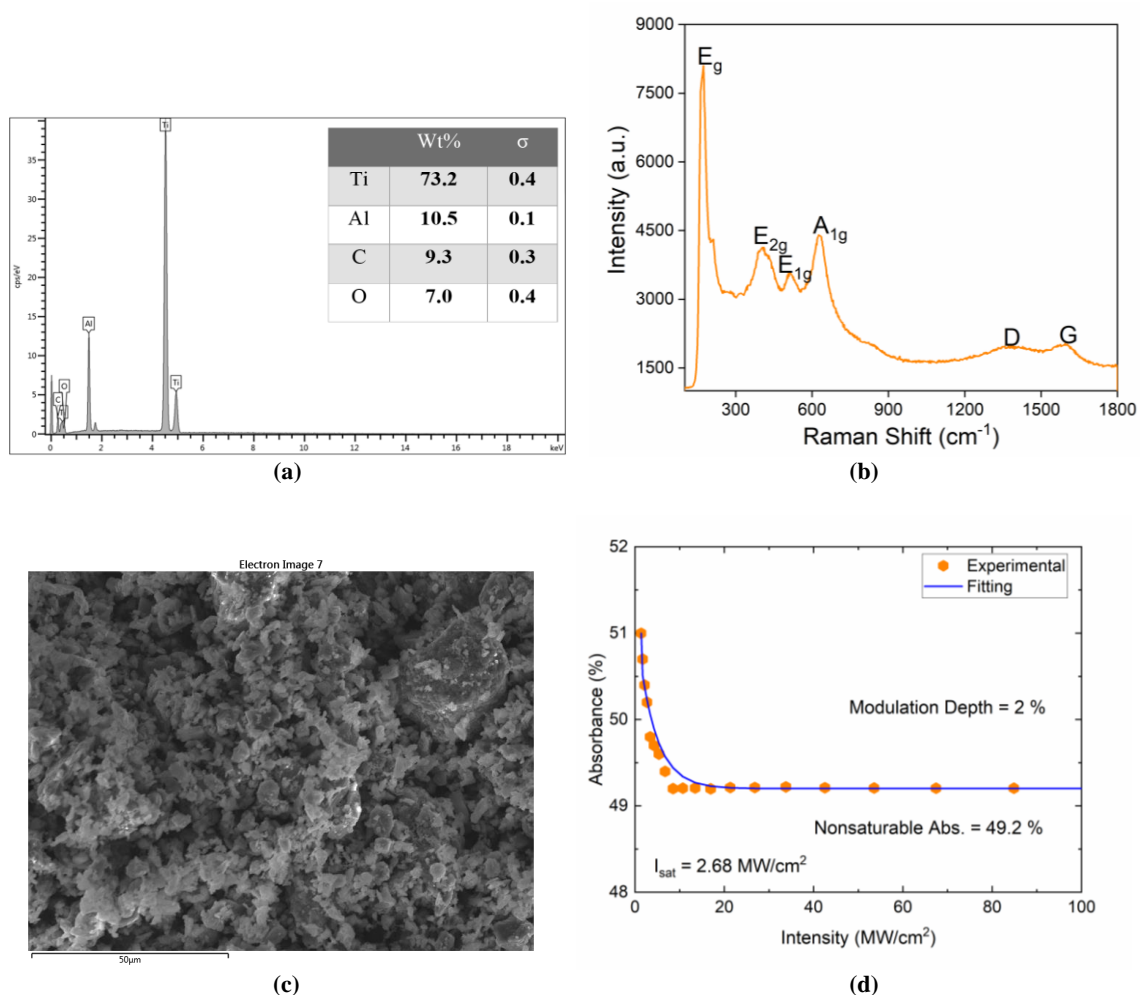


Figure 1. Characterization of Ti_3AlC_2 ; (a) EDS spectrum, (b) Raman spectrum, (c) VP-SEM image, and (d) nonlinear absorption profile at 1.55- μm region.

3. Experimental configuration for a dual-wavelength pulsed generation in an EDFL cavity

The EDFL cavity with the combination of optical components was developed to investigate the potential of MAX-DSF as SA device. As illustrated in Figure 2, the laser diode (LD) emitted at the 980 nm was used to obtain an excitation of energy in the laser configuration.

The light passed through the wavelength division multiplexer (WDM) with two input ports, and one of the ports was directly spliced to the LD. Then, the light travelled towards an erbium-doped fiber (EDF) to initiate the stimulated emission that works in the 1.55- μm regime. The EDF owns a 2.4 m length, an absorption coefficient of 23.9 dB/m, a numerical aperture of 0.24, and a core/cladding diameter of 9/125 μm . The light was forced to propagate in one direction via an optical coupler, with 20% extracted from the cavity for analysis purposes. The remaining 80% continues to travel inside the laser configuration. The optical coupler was spliced to a 100 m single-mode fiber (SMF-28) to lengthen the cavity. Finally, all the light hits the MAX-DSF, which stabilized the ultrashort pulse. The measuring instruments used were the digital oscilloscope (GWINSTEK, GDS3352), optical spectrum analyzer (ANRITSU, MS9710C), radio frequency spectrum analyzer (7.8 GHz ANRITSU, MS2683A), and optical power meter. The oscilloscope and radio frequency spectrum analyzer were connected to the cavity via an InGaAs photodetector. The total cavity length was 114.6 m.

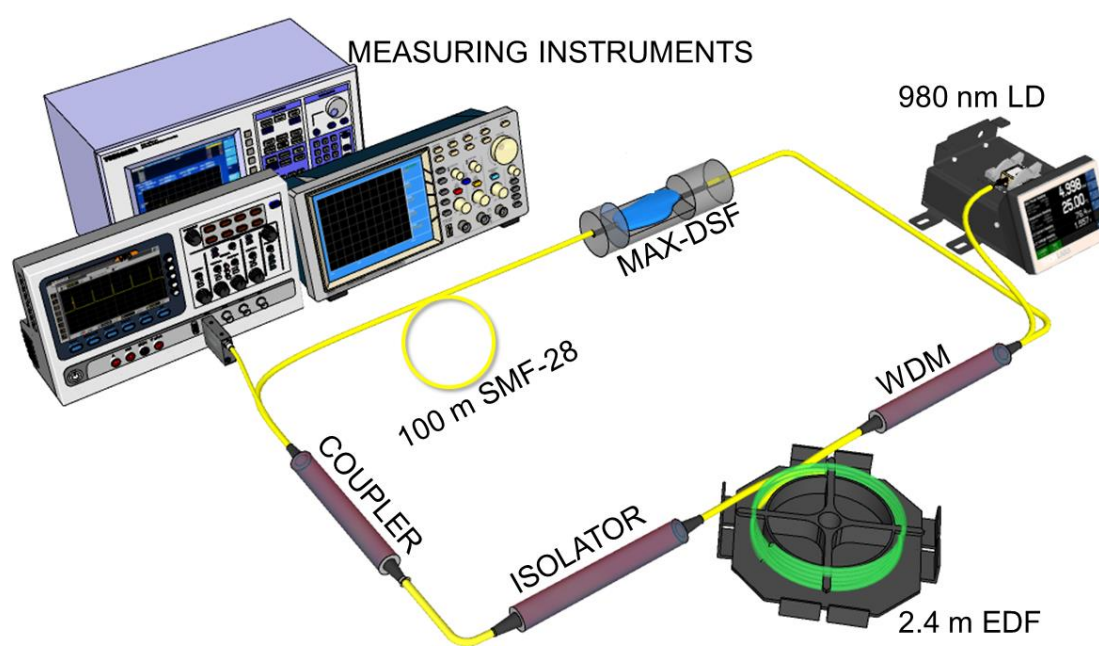


Figure 2. Experimental configuration for dual-wavelength pulse generation in an EDFL cavity.

4. The generation of dual-wavelength laser with Ti_3AlC_2 deposited onto D-shaped fiber

The assembled laser configuration emits a continuous-wave (CW) laser at the pump power of 16 mW. The generation of the CW regime was proven by the captured OSA spectrum with a central wavelength of 1560 nm, as shown in Figure 3 (a). Next, the MAX-DSF SA triggered a DWL generation at the threshold pump power of 62 mW. The spectrum in Figure 3 (a) shows two peaks located at the wavelength of 1533 nm and 1557 nm. A typical blue shift of center wavelength indicates the modulation of loss by the SA incorporated inside the EDFL cavity. This phenomenon also occurred because of the laser cavity's behavior to obtain a higher gain to compensate for that loss. By tuning the input power from 62 to 90 mW, the stable DWL laser was sustained without any noticeable pulse destruction. Figure 3 (b) depicts the oscilloscope trace of DWL laser at the highest input power of 90 mW. Slight amplitude fluctuation of the sinusoidal waves comes from the timing jitter's presence, which was attributed to the low intracavity pulse energy in the laser configuration [15]. As observed in Figure 3 (b), the two waveforms own a crest-to-crest distance of 530 ns while the full-width

half-maximum (FWHM) measured for a single pulse was 280 ns. A radio frequency (RF) spectrum was captured within a 3 MHz frequency to confirm the stability of the generated DWL, as shown in Figure 3 (c). The frequency obtained at the fundamental peak was 1.887 MHz. This value corresponds to the pulse period captured at the oscilloscope trace, which was 530 ns. The signal-to-noise ratio (SNR) of ~63 dB indicates an ML laser with a low resonant relaxation oscillation frequency [16]. The cavity length of 114.6 m agreed with the repetition rate of 1.887 MHz, and it corresponds with the total round-trip time of the cavity (530 ns).

A nearly uniform repetition rate within the input power of 62 to 90 mW indicated a stable operation of DWL laser. The laser emits the repetition rate with a standard deviation of 0.000535 MHz, calculated between the value of 1.887-1.888 MHz. The variation of pump power between 62-90 mW generates the pulse width of 277-281 ns with a standard deviation of 1.5119 ns, suggesting a consistent pulsed laser. The output characteristics of the generated pulsed laser were obtained with an optical power meter. This measurement yields a graph in Figure 3 (d). First, the chart shows output power captured as the pump power adjusted from 62 to 90 mW, with the maximum value obtained was 4.4 mW. The slope efficiency calculated from its gradient depicted a high-power conversion efficiency of 6.5%. The pulse energy and peak power recorded were linearly increased with the increase in pump power, as illustrated in Figure 3 (d). The maximum attainable pump power of ML (90 mW) gives the highest pulse energy of 2.33 nJ and peak power of 8.33 mW. The outstanding output characteristics indicate a low loss laser cavity and the SA device with excellent nonlinear absorption properties.

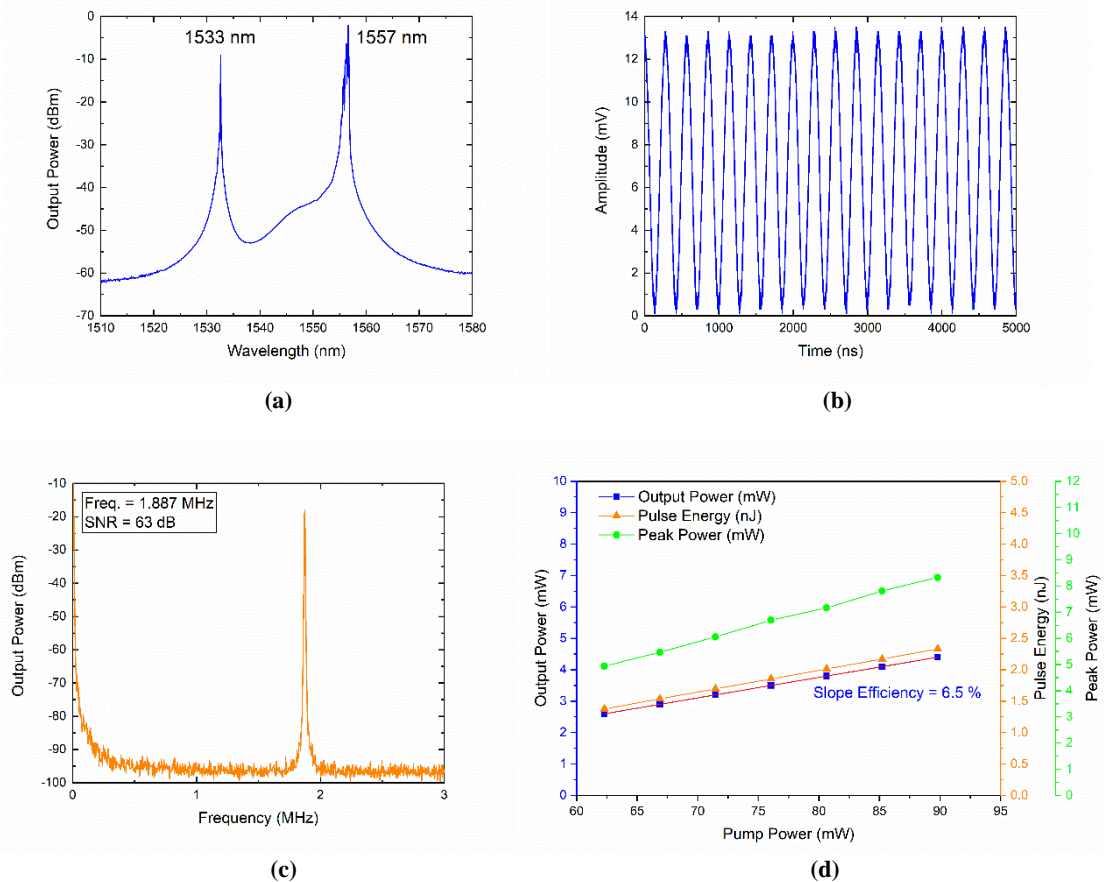


Figure 3. Performance of dual-wavelength mode-locked laser; (a) optical spectrum, (b) oscilloscope spectrum, (c) radio frequency spectrum, and (d) the graph of output power, pulse energy, and peak power as a function of pump power.

5. Conclusion

In conclusion, the works show a potential of MAX phase Ti_3AlC_2 as a saturable absorber operates in the 1.55- μm regime. A few drops of liquid Ti_3AlC_2 have successfully expressed the evanescent field interaction on the surface of the D-shaped fiber. Further, by incorporating the SA device into the EDFL cavity, a stable dual-wavelength mode-locked laser was generated. This laser emits an output centered at 1533 nm and 1557 nm as the pump power tuned from 62 to 90 mW. The pulse width and repetition rate obtained was 280 ns and 1.887 MHz at the highest input power of 90 mW. The findings also suggest an option to the thin-film structure of the SA device, as the developed MAX-DSF owns a modulation depth of 2%, which was comparable to its thin-film counterparts. The first demonstration of the dual-wavelength mode-locking generation by using MAX phase coated D-shaped fiber opens a new pathway towards versatile SA in an all-fiber based laser cavity.

Acknowledgement

This work was financially supported by the Malaysian Ministry of Higher Education (MOHE) under the Fundamental Research Grant Scheme (FRGS), R.J130000.7854.5F183. The authors would also like to thank the Department of Physics, Universiti Teknologi Malaysia for the research facility provided throughout this work.

References

- [1] Li S, Wang C, Yin Y, Lewis E and Wang P 2020 Novel layered 2D materials for ultrafast photonics 20200030
- [2] Novoselov K S, Geim A K, Morozov S V, Jiang D, Zhang Y, Dubonos S V, Grigorieva I V and Firsov A A 2004 Electric field effect in atomically thin carbon films *Science* **306** 666-9
- [3] Bao Q L, Zhang H, Wang Y, Ni Z H, Yan Y L, Shen Z X, Loh K P and Tang D Y 2009 Atomic-Layer Graphene as a Saturable Absorber for Ultrafast Pulsed Lasers *Adv. Funct. Mater.* **19** 3077-83
- [4] Chernysheva M, Mou C, Arif R, AlAraini M, Rümmele M, Turitsyn S and Rozhin A 2016 High Power Q-Switched Thulium Doped Fibre Laser using Carbon Nanotube Polymer Composite Saturable Absorber *Scientific Reports* **6** 24220
- [5] Li D A, Jussila H, Karvonen L, Ye G J, Lipsanen H, Chen X H and Sun Z P 2015 Polarization and Thickness Dependent Absorption Properties of Black Phosphorus: New Saturable Absorber for Ultrafast Pulse Generation *Scientific Reports* **5** 9
- [6] Chen B H, Zhang X Y, Wu K, Wang H, Wang J and Chen J P 2015 Q-switched fiber laser based on transition metal dichalcogenides MoS_2 , $MoSe_2$, WS_2 , and WSe_2 *Optics Express* **23** 26723-37
- [7] Duan L N, Wang Y G, Xu C W, Li L and Wang Y S 2015 Passively Harmonic Mode-Locked Fiber Laser With a High Signal-to-Noise Ratio via Evanescent-Light Deposition of Bismuth Telluride (Bi_2Te_3) Topological Insulator Based Saturable Absorber *IEEE Photonics J.* **7** 7
- [8] Jiang X T, Liu S X, Liang W Y, Luo S J, He Z L, Ge Y Q, Wang H D, Cao R, Zhang F, Wen Q, Li J Q, Bao Q L, Fan D Y and Zhang H 2018 Broadband Nonlinear Photonics in Few-Layer MXene Ti_3C_2Tx ($T = F, O, \text{ or } OH$) *Laser Photon. Rev.* **12** 10
- [9] Feng J J, Li X H, Feng T C, Wang Y M, Liu J and Zhang H 2020 An Harmonic Mode-Locked Er-Doped Fiber Laser by the Evanescent Field-Based MXene Ti_3C_2Tx ($T = F, O, \text{ or } OH$) Saturable Absorber *Annalen Der Physik* **532** 7
- [10] Jhon Y I, Koo J, Anasori B, Seo M, Lee J H, Gogotsi Y and Jhon Y M 2017 Metallic MXene Saturable Absorber for Femtosecond Mode-Locked Lasers *Adv. Mater.* **29** 1702496

- [11] Lee J, Kwon S and Lee J H 2019 Ti₂AlC-based saturable absorber or passive Q-switching of a fiber laser *Optical Materials Express* **9** 2057-66
- [12] Jiang X, Li W, Hai T, Yue R, Chen Z, Lao C, Ge Y, Xie G, Wen Q, Zhang H J n D M and Applications 2019 Inkjet-printed MXene micro-scale devices for integrated broadband ultrafast photonics **3** 1-9
- [13] Lokman M Q, Yusoff S, Ahmad F, Zakaria R, Yahaya H, Shafie S, Rosnan R M and Harun S W 2018 Deposition of silver nanoparticles on polyvinyl alcohol film using electron beam evaporation and its application as a passive saturable absorber *Results Phys.* **11** 232-6
- [14] Presser V, Naguib M, Chaput L, Togo A, Hug G and Barsoum M W 2012 First-order Raman scattering of the MAX phases: Ti₂AlN, Ti₂AlC_{0.5}N_{0.5}, Ti₂AlC, (Ti_{0.5}V_{0.5})₂AlC, V₂AlC, Ti₃AlC₂, and Ti₃GeC₂ **43** 168-72
- [15] Paschotta R 2010 Timing jitter and phase noise of mode-locked fiber lasers *Optics Express* **18** 5041-54
- [16] Yue W, Wang Y, Xiong C-D, Wang Z-Y and Qiu Q 2013 Intensity noise of erbium-doped fiber laser based on full quantum theory *J. Opt. Soc. Am. B* **30** 275-81